clear oscillations were observed, indicating a two-dimensional layer-by-layer growth mode. On the BHF-treated substrate (curve B), the oscillation was quite regular and the signal intensity recovered to the value of the original surface at each peak. The oscillation persisted more than 300 cycles. This film exhibited a terraced surface in the AFM image similar to that of Fig. 1B. The AFM image in Fig. 5 represents the surface of the film quenched at the bottom of the RHEED oscillation. The film surface showed 0.4-nm-high islands randomly distributed on the atomically flat terraces. The film surface quenched at the peak of the RHEED oscillation showed the atomically flat surface similar to Fig. 1B. These results demonstrate that the RHEED oscillation during homoepitaxy of $SrTiO_3$ indeed originates from the oscillation of the atomic scale surface roughness due to the two-dimensional layer-by-layer growth. When the film was deposited at temperatures higher than 780°C, the homoepitaxy proceeds in a step-flow mode, in which the RHEED signal did not oscillate, but the film surface was well terraced on an atomic scale. The film growth on the commercial substrates did not show any step structures and gave rapidly damping RHEED oscillations (*12*).

For further examining the applicability of the BHF-treated substrates, such perovskite-type materials as $PrGaO_3$ and $BaTiO_3$ were heteroepitaxially grown by laser MBE to give a clear RHEED oscillation and atomically flat and well-terraced surfaces. When $YBa_2Cu_3O_{7-\delta}$ was grown on this terraced clean substrate, the film surfaces exhibited terraces and steps one unit cell in height aligned in one direction. Such results could not be obtained for the films deposited on the commercial substrates (*13*, *14*). Thus, the BHF-treated substrates enable atomically regulated epitaxy of oxides comparable to that of semiconductors.

REFERENCES

1. J. G. Bednorz and K. A. Müller, *Z. Phys. B.* **64**, 189 (1986).
2. H. Koinuma *et al.*, *J. Appl. Phys.* **62**, 1524 (1987).
3. H. Koinuma, H. Nagata, T. Tsukahara, S. Gonda, M. Yoshimoto, *Appl. Phys. Lett.* **58**, 2027 (1991).
4. T. Terashima *et al.*, *Phys. Rev. Lett.* **65**, 2684 (1991).
5. See, for example, H. Koinuma, *Mater. Res. Soc. Bull.* **19**, 21 (September 1994).
6. M. Yoshimoto, H. Ohkubo, N. Kanda, H. Koinuma, *Jpn. J. Appl. Phys.* **31**, 3664 (1992).
7. T. Terashima *et al.*, *ibid.* **28**, L987 (1989).
8. S. Watanabe, T. Hikita, M. Kawai, *J. Vac. Sci. Technol.* **A9**, 2394 (1991).
9. M. Yoshimoto *et al.*, *Mater. Res. Soc. Symp. Proc.* **341**, 133 (1994).
10. M. Kawai *et al.*, *Appl. Surf. Sci.*, in press.
11. S. Gonda, H. Nagata, M. Kawasaki, M. Yoshimoto, H. Koinuma, *Physica* **C216**, 160 (1993).
12. M. Yoshimoto *et al.*, *Appl. Phys. Lett.* **61**, 2659 (1992).
13. J. P. Gong *et al.*, *Jpn. J. Appl. Phys.* **32**, L687 (1993).
14. M. Kawasaki *et al.*, *ibid.*, p. 1612.

22 August 1994; accepted 12 October 1994

Meltwater Input to the Southern Ocean During the Last Glacial Maximum

Aldo Shemesh, Lloyd H. Burckle, James D. Hays

Three records of oxygen isotopes in biogenic silica from deep-sea sediment cores from the Atlantic and Indian sectors of the Southern Ocean reveal the presence of isotopically depleted diatomaceous opal in sediment from the last glacial maximum. This depletion is attributed to the presence of lids of meltwater that mixed with surface water along certain trajectories in the Southern Ocean. An increase in the drainage from Antarctica or extensive northward transport of icebergs are among the main mechanisms that could have produced the increase in meltwater input to the glacial Southern Ocean. Similar isotopic trends were observed in older climatic cycles at the same cores.

During the past three decades, some of the most fundamental observations regarding past climate change and the changing chemical properties of seawater have been based on oxygen isotope analyses of calcium carbonate shells of foraminifera (*1–3*). Questions of importance to paleoclimatology and paleoceanography—on such topics as ice volume changes, the temporal and spatial distribution of meltwater pulses, and the tempo and mode of glacial-interglacial climate change—have been successfully addressed. Disintegration of major continental ice sheets and the consequent occurrence of large meltwater plumes during Northern Hemisphere deglaciation were inferred from $\delta^{18}O$ records from continental margin sediments (*4–7*) and sea level changes (*8*). All major meltwater discharge pulses into the Gulf of Mexico and other Northern Hemisphere regions (although not isochronous) are associated with deglaciation. These pulses have also imposed global changes in deep-water formation, in primary production, and in gas exchange between the ocean and the atmosphere. In the Southern Ocean, the presence of meltwater was inferred by indirect measurements of $^{231}Pa/^{230}Th$ in sediments and paleonitrate proxies (*9*) and also by a combination of foraminiferal $\delta^{18}O$ and diatom transfer functions (uncorrected for dissolution effects) in the Indian sector (*10*).

Although isotopic determination of foraminiferal calcium carbonate is applicable in marine sediments from low and mid-latitudes, it frequently has only marginal application in high-latitude regions such as the Southern Ocean because foraminiferal carbonate is frequently absent or present only in low concentrations in such regions. Recently, the use of oxygen isotopes of biogenic opal ($\delta^{18}O_{Si}$) secreted by marine diatoms was shown to provide paleoceanographic information that is complementary to that derived from foraminiferal $\delta^{18}O$ (*11*, *12*). Thus, the thermal history of the surface water of the Southern Ocean and meltwater input to this region can be identified and used to reconstruct ice dynamics around Antarctica. Because global climate change is the sum of local and regional climate change, the ability to recover oxygen isotope records from high southern latitudes provides a better understanding of global climate change.

South of the Polar Front zone (PFZ), diatoms are the dominant photosynthetic algae. They are light-limited, live within the uppermost layer of surface water, and secrete an opaline skeleton with known isotopic fractionation. Therefore, biogenic opal accumulating on the sea floor should reflect the temperature and isotopic composition of seawater at or near the sea surface at the time of deposition and can be used to reconstruct past variations in surface water properties. Earlier studies in sediments of the Weddell Sea and South Atlantic (*12*, *13*) have shown that diatom $\delta^{18}O$ records exhibit the predicted variation between glacials and interglacials. During glacial maxima, sea surface temperature is lower, and there is an increase in continental ice volume that preferentially removes ^{16}O from the ocean. Therefore, the content of ^{18}O in the solid phase in both foraminiferal carbonate and diatom opal is higher (*1*, *11*). Global warming and the melting of continental ice during interglacials produces ^{18}O minima in opal and carbonate during interglacials.

In this report, we describe and evaluate $\delta^{18}O_{Si}$ determinations from three deep-sea cores recovered from south of the PFZ in the Atlantic and Indian sectors of the Southern Ocean (Table 1). In these cores, diatom samples from the last glacial maximum (LGM) (about 18,000 years ago) exhibit light $\delta^{18}O_{Si}$ values; because temperatures should have been lower during the LGM, this result is contrary to the expectation that

A. Shemesh, Department of Environmental Sciences and Energy Research, The Weizmann Institute of Science, Rehovot, 76100, Israel.
L. H. Burckle and J. D. Hays, Lamont-Doherty Earth Observatory of Columbia University, Palisades, NY 10964, USA.

the most enriched isotopic values should occur in samples from this interval. We examined the possible cause of this depletion and demonstrate that localized meltwater lids over the surface of the Southern Ocean were present during the LGM.

Diatoms were separated from bulk sediment and prepared for analysis (*13*). An age model for each core is based on the relative abundance stratigraphy of *Cycladophora davisiana* (radiolarian) and *Eucampia antarctica* (diatom); these are the main stratigraphic markers in sediments of late Quaternary age from this region (*14–16*). Isotopic stage 2 (the level of the LGM) is well constrained by both markers in all cores. However, because there is no absolute age determination for these regions, there is always the possibility that age assignments based on biostratigraphy are in error.

The down-core diatom $\delta^{18}O_{Si}$ records indicate that stage 2 was characterized by light $\delta^{18}O_{Si}$ values, in contrast to the expected isotopic signal for the LGM period. The RC11–94 record (Fig. 1) reveals that the light $\delta^{18}O_{Si}$ values were confined to the earlier part of stage 2. The sedimentation rates in two of the cores, RC11–97 (Fig. 2) and RC13–259 (Fig. 3), were low during stage 2, and therefore, it is difficult to determine if the light $\delta^{18}O_{Si}$ occurred at the bottom or top of the glacial section. However, the general trend of light $\delta^{18}O_{Si}$ values associated with high percentages of *C. davisiana* and *E. antarctica* is seen not only in stage 2 but in older glacial stages as well.

We attribute variations in $\delta^{18}O_{Si}$ to conditions that prevailed in surface waters during stage 2. On the basis of other $\delta^{18}O_{Si}$ records from the Southern Ocean (*12, 13*), the possibility that light $\delta^{18}O_{Si}$ values are an artifact of post-depositional alteration, preferential dissolution, or species composition is discounted because isotopic alteration was not observed in such sediments. Two variables, temperature and $\delta^{18}O$ of seawater, can produce the observed isotopic shifts. A warming of surface water by 4° to 7°C between stage 3 and stage 2 would have been required if the record reflects temperature changes. However, such warming contradicts results from all temperature proxies in these regions (*14, 17*) and is unlikely to have occurred at the time of global cooling and both ice sheet and sea ice expansion toward the north. A change in the $\delta^{18}O$ value of surface seawater could only have been achieved by an influx of meltwater originating from continental ice or snow, which have low $^{18}O/^{16}O$ ratios. The formation and melting of sea ice are associated with small isotopic fractionation (*18*) and therefore cannot account for an isotopic

Table 1. Core locations and water depths.

Core	Latitude	Longitude	Water depth (m)
RC13-259	53.88°S	4.93°W	2677
RC11-94	54.48°S	53.05°E	4303
RC11-97	50.32°S	61.20°E	4638

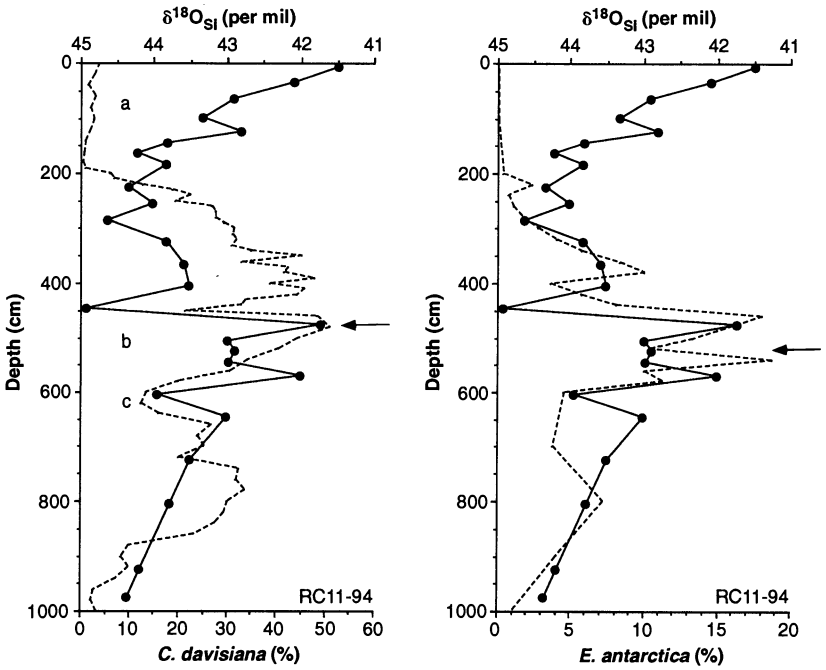

Fig. 1. Down-core variation of diatom $\delta^{18}O_{Si}$ (solid line) and percent *C. davisiana* (dashed line, left figure) and percent *E. antarctica* (dashed line, right figure) in the Indian Ocean core RC11–94. The arrow indicates the position of the LGM level in the core according to these two biostratigraphic markers; radiolarian zones a, b, and c correspond to isotopic stages 1, 2, and 3, respectively. The depleted isotopic values are associated with the cold isotopic stage 2. The Holocene (interval between 180 and 0 cm) gradual depletion in $\delta^{18}O_{Si}$ was previously observed in other Atlantic deep-sea cores (*13*).

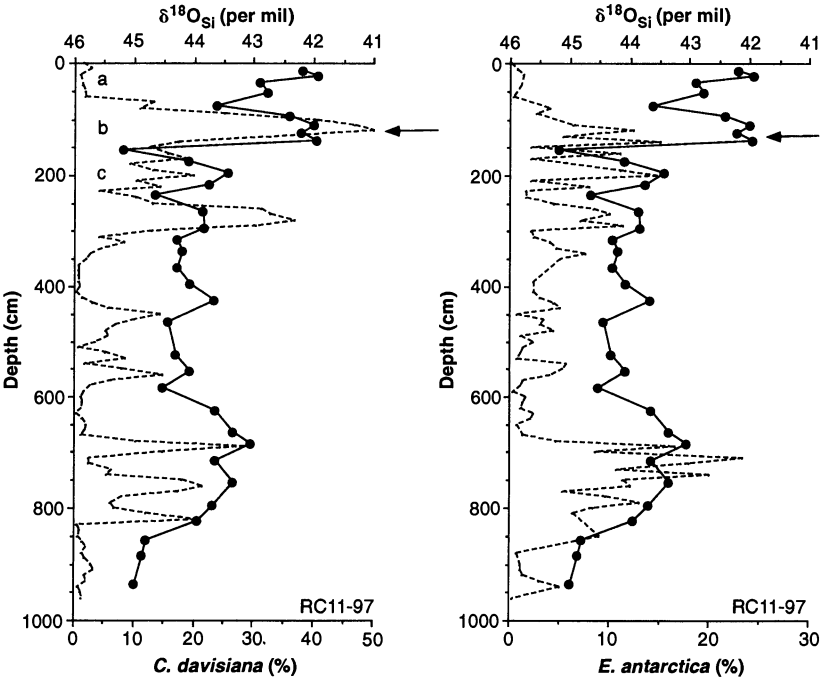

Fig. 2. Down-core variation of diatom $\delta^{18}O_{Si}$ (solid line) and percent *C. davisiana* (dashed line, left figure) and percent *E. antarctica* (dashed line, right figure) in the Indian Ocean core RC11–97. The arrow and radiolarian zones are as in Fig. 1. The depleted isotopic values are associated with the cold isotopic stage 2 and with stage 6 at a depth of 700 cm. The Holocene depletion (60 to 0 cm) is present but with a reduced amplitude because of the low sedimentation rate.

change of 2 per mil in surface waters. Possible sources of ^{18}O-depleted meltwater to the Southern Ocean are the bottom melting of ice shelves or the melting of icebergs and snow that accumulated on sea ice.

We cannot estimate the relative importance of these possible sources in the production of the observed signal. However, the observation that the anomalous records are confined to certain localities in the southern Atlantic and Indian oceans sugests that the input of meltwater must reflect a local phenomenon such as iceberg melting along certain trajectories or increased input from several Antarctic outlets. Ice sheet studies (*19–22*) in East and West Antarctica and on coastal terraces around Antarctica reveal fluctuations in the flow of ice and meltwater that would be capable of causing the observed isotopic records. The amount of mixing between seawater and meltwater to produce an opal depletion of 2 per mil during stage 2 can be calculated by isotopic mass balance. Taking −35 per mil as an average $\delta^{18}O$ value for continental ice (*23*), we obtain a mix of 94% seawater and 6% meltwater, which corresponds to a reduction of 2 per mil in surface water salinity. The total amount of meltwater addition to the Southern Ocean cannot be calculated at this point because the depth of the mixed layer and its spatial distribution are still unknown.

Our conclusion that a meltwater lid occurred during the LGM in parts of the Southern Ocean is supported by biotic evidence. Percent abundance of the diatom *E. antarctica* is largely driven by changes in absolute abundance of open ocean diatoms. However, there is little change in abundance of *E. antarctica* in the cores between the interglacial and glacial sediments. We conclude that the productivity of open ocean diatoms is suppressed by the presence of sea ice and meltwater lids during glacial maxima.

Mid-Holocene glacial expansion of the major outlet systems in East Antarctica was reported to be associated with periods of warming (*24*). Large changes in the Lambert glacier system occurred during the mid-Holocene (*25*). The exact expansion of the LGM East Antarctic ice sheet and shelves is uncertain. The Holocene data indicate a dynamic system affecting sea level and drainage rates on short and long time scales. We suggest that fluctuations in ice expansion can be one of the main factors controlling meltwater lids during the LGM. Although the increase in meltwater output occurred during the coldest period when the precipitation of the ice sheet was reduced, the cause for the change in drainage output through time remains unknown and is not necessarily associated with air temperature. Other factors that involve isostatic response and ice stability might be of major importance. Alternatively, meltwater lids during the LGM could have been produced solely by iceberg melting. Sea ice protects icebergs from erosion by waves, and so, increased sea ice cover during the LGM would have allowed the northward penetration of icebergs that could have melted during the probably short summer. This would have concentrated meltwater in both time and space during glacial maxima. Information concerning the ice-volume state of Antarctic glacial systems during the late Pleistocene through the Holocene and an independent evaluation of Antarctic coasts to correlate between the continental record and the marine record in the Southern Hemisphere are needed to unravel the exact mechanism that produced meltwater lids during the LGM.

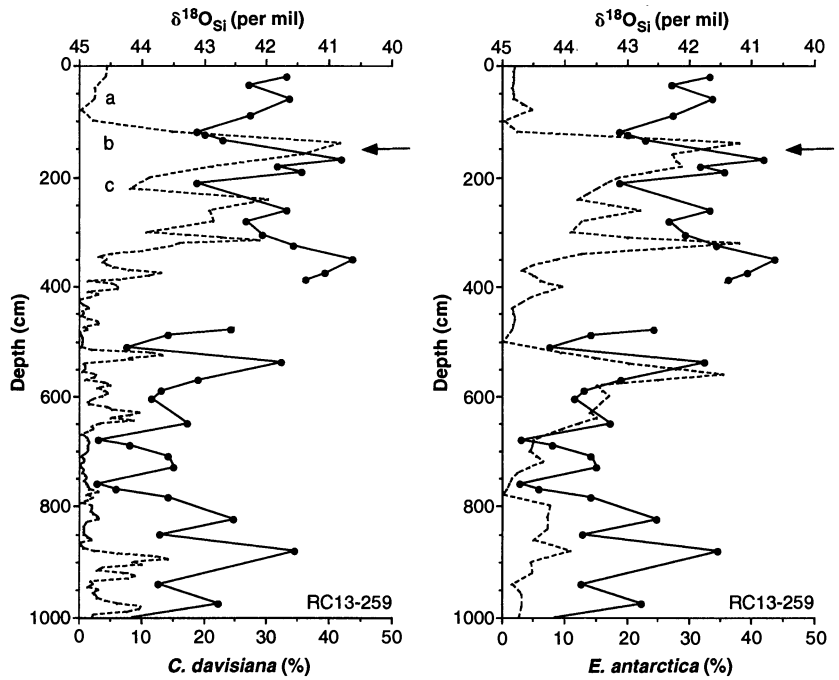

Fig. 3. Down-core variation of diatom $\delta^{18}O_{Si}$ (solid line) and percent *C. davisiana* (dashed line, left figure) and percent *E. antarctica* (dashed line, right figure) in the Atlantic Ocean core RC13-259. The arrow and radiolarian zones are as in Fig. 1. Depleted values of $\delta^{18}O_{Si}$ covary with high counts of *C. davisiana* and *E. antarctica* in the core. Samples from 400 to 500 cm were not available for $\delta^{18}O_{Si}$ determinations. The bottom of the core corresponds to isotopic stage 12.

REFERENCES AND NOTES

1. C. Emiliani, *J. Geol.* **63**, 538 (1955). All isotopic data are reported in the δ notation: $\delta^{18}O = 1000 (R_{sample}/R_{standard} - 1)$, where $R = {}^{18}O/{}^{16}O$.
2. N. J. Shackleton, *Quat. Sci. Rev.* **6**, 183 (1987).
3. ——— and N. D. Opdyke, *Quat. Res.* **3**, 39 (1976).
4. J. P. Kennett and N. J. Shackleton, *Science* **188**, 147 (1975).
5. A. Leventer, D. F. Williams, J. P. Kennett, *Earth Planet. Sci. Lett.* **59**, 11 (1982).
6. W. S. Broecker *et al.*, *Radiocarbon* **32**, 119 (1990).
7. G. Jones and L. D. Keigwin, *Nature* **336**, 56 (1988).
8. R. G. Fairbanks, *ibid.* **342**, 637 (1989).
9. R. Francois, M. P. Bacon, M. A. Altabet, L. D. Labeyrie, *Paleoceanography* **8**, 611 (1993).
10. L. D. Labeyrie *et al.*, *Nature* **322**, 701 (1986).
11. A. Juillet-Leclerc and L. D. Labeyrie, *Earth Planet. Sci. Lett.* **84**, 69 (1987).
12. A. Shemesh, C. D. Charles, R. G. Fairbanks, *Science* **256**, 1434 (1992).
13. A. Shemesh, L. H. Burckle, J. D. Hays, in preparation; the fluorination line is calibrated with the use of the NBS-20 standard of the National Bureau of Standards. Diatom $\delta^{18}O_{Si}$ values are reported versus the standard mean ocean water (SMOW) standard, and the long-term reproducibility is better than 0.14 per mil for diatom samples.
14. J. D. Hays, J. A. Lozano, N. J. Shackleton, G. Irving, *Geol. Soc. Am. Mem.* **145**, 337 (1976).
15. L. H. Burckle and D. W. Cooke, *Micropaleontology* **29**, 6 (1983).
16. D. W. Cooke and J. D. Hays, in *Antarctic Geoscience*, C. Craddock, Ed. (Univ. of Wisconsin Press, Madison, WI, 1982), pp. 1017–1025.
17. CLIMAP Project Members, *Geological Society of Amenca. Map and Chart Service, MC 36* (1981).
18. R. F. Weiss, H. G. Ostlund, H. Craig, *Deep-Sea Res. A* **26**, 1093 (1979).
19. R. G. Johnson and J. T. Andrews, *Paleoceanogr. Paleoclimatol. Paleoecol.* **53**, 107 (1986).
20. M. Nakada and K. Lambeck, *Nature* **333**, 36 (1988).
21. D. R. MacAyeal, *ibid.* **359**, 29 (1992).
22. E. A. Colhoun, M. C. G. Mabin, D. A. Adamson, R. M. Kirk, *ibid.* **358**, 316 (1992).
23. S. S. Jacobs, R. G. Fairbanks, Y. Horibe, in *Oceanology of the Antarctic Continental Shelf*, S. S. Jacobs, Ed. (American Geophysical Union, Washington, DC, 1985), pp. 59–85.
24. E. W. Domak, A. J. T. Jull , S. Nakao, *Geology* **19**, 1059 (1991).
25. N. F. McIntyre, *J. Glaciol.* **31**, 34 (1985).

26. We thank the curator of Lamont-Doherty Earth Observatory for providing the samples. This work was supported by a grant of the Israel Academy of Science and Humanities to A.S. and by a grant of the Office of Polar Programs (OPP 92–20216) to L.H.B.

30 June 1994; accepted 26 September 1994